First-principles investigation of hydrogen embrittlement in polycrystalline Ni_3Al

Wang Fuhe and Wang Chongyu
CCAST (World Laboratory), P.O. Box 8730, Beijing 100080, People's Republic of China
and Central Iron and Steel Research Institute, Beijing 100081, People's Republic of China
(Received 27 January 1997; revised manuscript received 21 September 1997)

The discrete-variational method within the framework of density-functional theory is used to study the effect of hydrogen on the embrittlement of polycrystalline Ni_3Al. The calculated results of impurity formation energy show that hydrogen atoms prefer to segregate at the grain boundaries, and occupy the Ni-rich interstitial holes in the polycrystalline Ni_3Al. The equilibrium positions of H atoms are near a certain atom instead of the center of these holes. The calculated results of interatomic energies reveal that the bonding strength of host atoms, which are near hydrogen atoms, are reduced evidently by the presence of hydrogen. The overall effect of H is to decrease the cohesive strength of Ni_3Al grain boundaries and make intergranular fracture easier. [S0163-1829(98)09101-2]

I. INTRODUCTION

As a high-temperature structural material, Ni_3Al has many attractive properties such as high-temperature strength, low density, resistance to oxidation, etc. However, brittle grain-boundary fracture is the major problem of polycrystalline Ni_3Al for the use of mechanics.[1] Traditionally, the grain boundaries in Ni_3Al were concluded to be intrinsically brittle. However, recent work from Liu *et al.*[2–6] has shown that the extrinsic fracture, environmental embrittlement, is a major cause of low ductility and brittle intergranular fracture in binary Ni_3Al.

Several mechanisms have been proposed to explain hydrogen embrittlement in non-hydride-forming metals and alloys.[7,8] Basically, the theories fall into two categories. The first is the decohesion mechanism, which was originally proposed for steel by Troiano[9] and modified by Oriani and Josephic.[10] In this mechanism, they suggested that hydrogen reduces the cohesive force between the atoms and thus promotes brittle fracture by bond rupture. The second class of mechanism is based on the premise that hydrogen affects the behavior of the dislocation emission at the crack tip area.[11] Beachem[11] and later Robertson and Birnbaum[12] proposed that hydrogen enhances the plasticity in front of the crack tip by lowering the flow stress. Lynch[13] argued that hydrogen chemisorbed at the crack tip lowers the stress which is necessary to operate near-surface dislocation sources and results in transgranular crack growth. However, as stated by Hirth,[7] simple mechanisms as mentioned above are not sufficient to rationalize the general degradation in properties produced by hydrogen.

There are several experimental studies on the hydrogen embrittlement in binary Ni_3Al,[2,4–6,14] $Ni_3(Al,Mn)$,[15] $Ni_3(Al,Zr)$,[3] and boron-doped Ni_3Al.[14,16–21] George *et al.* studied the environmental effect in polycrystalline Ni_3Al, which was carefully prepared from recrystallization of cold-worked single-crystal material, and found that the polycrystalline specimens exhibit a room-temperature tensile ductility of 3.1–4.8 % in air and 23% in ultrahigh vacuum. These results clearly demonstrate that binary Ni_3Al alloys are prone to environmental embrittlement at room temperature.[4–6] Masahashi *et al.*[15] found that $Ni_3(Al,Mn)$ has severe hydrogen embrittlement susceptibility, whether the hydrogen is the residual in the specimens or that penetrated from the environment. The sensitivity of ductility to the test environment of boron-doped Ni_3Al depends on the content of boron. When doped with 0.012 wt. % boron, the Ni_3Al is susceptible to environmental embrittlement;[17] but when doped with 0.05 wt.% boron, the tensile ductility of Ni_3Al is insensitive to test environment.[16] However, when precharged with hydrogen, the ductility and the ultimate tensile strength of boron-doped Ni_3Al is much decreased, and the fracture mode is changed from ductile transgranular to brittle intergranular, though the yield stress is not affected by hydrogen.[19,20] Furthermore, the hydrogen embrittlement is sensitive to the strain rate, it is less at the higher strain rate.[20,21]

The understanding of hydrogen embrittlement in Ni_3Al alloys is far from being complete.[20] Kuruvilla and Stoloff[19] proposed that hydrogen-assisted cracking in B-doped Ni-rich Ni_3Al is due to hydrogen increasing the stress concentration at grain boundary. On the other hand, Bond *et al.*[14] concluded from their transmission electron microscope observations that hydrogen counteracts the strengthening effect of boron on the grain boundary and reduces the cohesive strength of the grain boundaries. Recently, Li and Chaki[20,21] suggested that the hydrogen-enhanced localized plasticity near the crack tip is the hydrogen embrittlement mechanism in ductile Ni_3Al alloy. In addition, Wan *et al.*[18] studied the deformation and fracture characteristics of hydrogen-charged and uncharged Ni_3Al-B with scanning electron microscopy, and suggested that both grain-boundary decohesion and high stress concentration contribute to the hydrogen-assisted intergranular cracking in boron-doped Ni_3Al alloy.

The amount of quantum-theoretical information is limited by the complexity of the hydrogen embrittlement procedure including transport of hydrogen to the microcrack and concentration of hydrogen in the front of crack tip, etc.[22] Eberhart *et al.*[23,24] calculated the electronic structure of a Fe_4H_2 cluster using the multiple-scattering $X\alpha$ method with a small cluster model. It was suggested that the hydrogen-assisted ductility is induced by the dilute, noninteracting, hydrogen

atoms, while cleavage fracture is the result of high concentration of hydrogen at the crack tip. Tománek *et al.* studied the hydrogen embrittlement in palladium using pseudopotential formalism[25] and molecular-dynamics calculation.[26] It was found that the occupation of the Pd-5s band is decreased near hydrogen atoms, whereas the filling of the Pd-4d band is increased to a near-noble-metal configuration. The latter effect decreased the contribution of 4d electrons to anisotropic bonding, and then reduced the shear modulus and increased ductility. The local enhancement of ductility in hydrogen-saturated regions of metal will cause a reduction of the critical tensile stress at which failure occurred. Fu and Painter[27] studied the hydrogen embrittlement in bulk FeAl using the full-potential linearized augmented plane-wave and the atomic cluster methods. It was shown that the charge transferred from 3d of the Fe atom to the hydrogen atom decreases the Fe-Al cleavage (or cohesive) strength. Recently, Sun *et al.*[28] studied the effect of boron and hydrogen on the atomic bonding in bulk Ni_3Al by use of the full-potential linear muffin-tin orbital method. Their calculating results shown that both boron and hydrogen prefer to occupy octahedral interstitial sites that are entirely coordinated by six nickel atoms. Hydrogen is found to enhance the bonding-charge directionality near some Ni atom and reduce the interstitial charge. This indicates that hydrogen promoted poor local cohesion.

The purpose of this work is to understand the electronic mechanism of hydrogen-induced embrittlement in polycrystalline Ni_3Al. With this end, we used the discrete-variational method[29–34] (DVM) to study the effect of hydrogen on the electronic structure of grain boundaries in Ni_3Al.

II. COMPUTATION METHOD AND CLUSTER MODEL

The discrete-variational method (DVM), which is a first-principles numerical method for solving the local-density-functional equations,[29–34] has been used successfully to study the electronic structure of metals and alloys.[33,34] In this work, the DVM is used to study the effect of hydrogen on the electronic structure of the grain boundary in Ni_3Al.

In order to approach the bulk by a cluster model, the embedded-cluster model[33,34] is used. In constructing the self-consistent potential, the charge density of several hundreds of atoms surrounding the cluster is included. Localization of cluster orbitals due to the Pauli exclusion principle is simulated by truncating the external potential wells at the Fermi energy level E_F.[33]

In the one-electron wave equation, the Hamiltonian in Hartree atomic units is

$$H=-\nabla^2/2+V_c+V_{\mathrm{xc}}, \tag{1}$$

where V_c is the electron-nucleus and electron-electron Coulomb potential, and V_{xc} is derived by Von Barth and Hedin[35] is the exchange-correlation potential. The eigenstates (or molecular orbitals) are expanded as a linear combinations of atomic orbitals $\phi_i(r)$ (Refs. 29,34)

$$\psi_n(r)=\sum_i C_{ni}\phi_i(r). \tag{2}$$

In order to study the interaction between atoms, the interatomic energy between atom l and m is derived[36,37]

$$E_{lm}=\sum_n \sum_{\alpha\beta} N_n a^{\star}_{n\alpha l} a_{n\beta m} H_{\beta m\alpha l}, \tag{3}$$

where N_n is the occupation number for molecular orbital ψ_n, $a_{n\alpha l}=\langle \phi_{\alpha l}(r)|\psi_n(r)\rangle$, and $H_{\beta m\alpha l}$ is the Hamiltonian matrix element connecting the atomic orbital β of atom m and the atomic orbital α of atom l.

In the computation, the single-site orbitals are used as the basis set, consisting of Ni:$[1s2s2p3s3p]3d4s4p$, Al:$[1s2s2p]3s3p$, and H:$1s$. The orbitals in the square brackets are frozen-core orbitals. In order to induce bound excited states, the funnel-potential[31] is introduced. The non-spin-polarized secular equations are solved using the self-consistent-charge approximation.[30]

The grain boundary $\Sigma 13[001](320)$ which is constructed by use of the coincidence site lattice (CSL) model and atomistic simulations,[38] is investigated. Figure 1 shows the atomic configuration for $\Sigma 13$ grain boundary in Ni_3Al. In order to study the energies of the system when hydrogen atoms occupy different sites in the same $\Sigma 13$ grain boundary in Ni_3Al and keep the occupation sites of hydrogen atoms at the center region of the cluster, two clusters (model A and B) are used to model the structure of $\Sigma 13$ grain boundary. The cluster atoms symbolized by solids (in Fig. 1) are embedded in several hundreds of surrounding atoms, which are symbolized by hollows. Each cluster contains three layers in the X direction, and a period unit in the Z direction. The atoms in the middle layer, i.e., the YZ plane ($x=0$) are represented by large solid symbols, the upper ($x=0.5a$, where a is constant of Ni_3Al crystal) and lower ($x=-0.5a$) layers are represented by little solid symbols. Indeed, the stacking sequence along the X axis is $\cdots ABABAB\cdots$. Assuming the YZ plane ($x=0$) in the model A is A, then the YZ plane in the model B is B, and their interval distance is a half of the crystal constant of Ni_3Al. In order to discuss the interaction between atoms clearly, the atoms in the cluster are labeled with numbers. The possible occupation sites of hydrogen are labeled by $Xn(n=1-5)$ and discussed in the next section. When the grain boundary is constructed by the use of CSL, the shortest interatomic distance at the $\Sigma 13$ grain boundary is much shorter than that in Ni_3Al crystal, so the atomic relaxation at the grain boundary should be considered, and it is carried out by the energy minimization procedure.[37] After relaxation, these atoms, such as 2,4 and 3,5, and 23 and 24, etc., which have the shorter interatomic distance at grain boundary, are pulled apart 0.21 Å from the grain boundary.

In order to get the hydrogen occupation position in the crystalline Ni_3Al, another two embedded clusters (model A and B, each contain three neighbor shells of atoms, i.e., 43 atoms) are chosen to simulate all the possible interstitial surroundings in the Ni_3Al crystal. In these models, the occupation site (denoted by $X0$) of hydrogen is the octahedral interstice. The neighbor atoms of $X0$ are two Al atoms and four Ni atoms in model A, and six Ni atoms in model B, respectively.

To find the stable site of hydrogen in polycrystalline Ni_3Al, the impurity formation energies E_{imp} for the system containing n hydrogen atoms can be defined as the nth of the

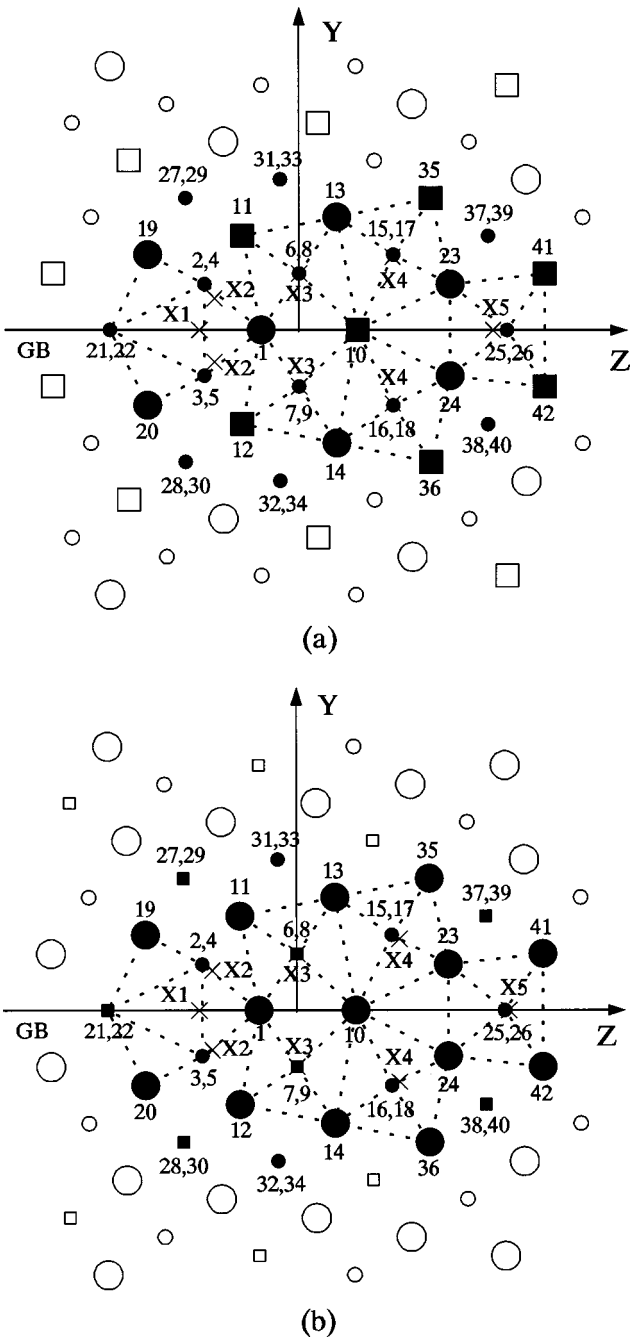

FIG. 1. The atomic configurations around $\Sigma 13[001](320)$ tilt grain boundaries in Ni_3Al. The Ni and Al atoms are represented by the circles and squares; the different sizes represent different layers, and the atoms shown as large symbols are in the YZ plane. The atoms shown as solid symbols and labeled by numbers are in the cluster, which is embedded by several hundreds of surrounding atoms (labeled by hollow symbols). The crosses labeled with Xn $(n=1-5)$ represent the possible occupation sites of hydrogen. (a) model A, (b) model B.

difference of the total energy between the hydrogen-containing system and the clean system. The magnitude of the impurity formation energy is, in general, of the order of a few electron volts, while total energy is of the order of 10^5 eV. In order to control numerical noise, E_{imp} can be obtained from the relative difference of the corresponding binding energies.

A total of 51 600 sample points for the self-consistent-field procedure were found to be sufficient for the 43-atom cluster. Uncertainties in binding energy are estimated as 0.05 eV/atom. We emphasize the relative change of system energy induced by the presentation of hydrogen and choose the same integral grid for the same model to calculate the E_{imp}, which is only related to one or two hydrogen atom(s) addition. So the relative accuracy of E_{imp} is about 0.1 eV, and it is high enough for the prediction of the hydrogen occupation site.

III. RESULTS AND DISCUSSION

A. The impurity formation energy of hydrogen

In order to get the lowest formation energies from all the possible interstitial sites, the coordinates of H occupation sites were changed symmetrically, and the corresponding formation energies were calculated. The formation energies for several possible occupation sites labeled by $Xn(n=0-5)$ are listed in Table I. $X0$ is the occupation site in the crystalline Ni_3Al. $X1-X5$ are the occupation sites in the grain boundary and locate in the YZ plane $(x=0)$. In the case of $X1$ and $X5$, there is only a single hydrogen atom in the cluster, respectively. However, there are a pair of hydrogen atoms (H_1 and H_2) in the cluster for the cases of $X2$, $X3$, and $X4$, and we assign that H_1 and H_2 locate at the upper $(Y>0)$ and lower $(Y<0)$ part of the grain boundary. $X1$ locates at the hole of the capped trigonal-prism, which is composed of No. 2,3,21,4,5, and 22 with the cap 1,19 and 20 atoms. In the $X2$ case, H_1 and H_2 locate near to the middle points between Ni_2 and Ni_4, Ni_3 and Ni_5, respectively. In the case of $X3$, H_1 and H_2 are in the hole of distorted octahedrons, which is composed of No. 1,10,13,11,6,8, and No.1,10,14,12,7,9 atoms, respectively. In the case of $X4$, H_1 and H_2 are in the hole of distorted octahedrons, which is composed of No. 10,23,35, 13,15,17, and No. 10,24,36,14,16,18 atoms, respectively. $X5$ is in the hole of distorted octahedron, which is composed of No. 23,24,42,41,25 and 26 atoms. These sites except $X3$ are not in the center of these interstitial holes, instead, the hydrogen atom tends to interact strongly with a certain atom. This behavior of hydrogen was also found in transition metals nickel and iron by theoretical calculation[39] and experimental measurement.[40] Furthermore, the coordinates of the corresponding sites in models A and B are slightly different owing to the different surrounding atoms.

Comparing the corresponding formation energies at sites $X0$, $X1$, $X2$, $X4$, and $X5$ in models A and B, it can be found that the formation energies at $X0$, $X2$, $X4$, and $X5$ in model B are lower than that in model A, in contrast, the formation energy at site $X1$ in model A is lower than that in model B. Noting the atomic type (Ni or Al) of neighboring atoms between the corresponding sites in the two models, it can be found that hydrogen atoms prefer to occupy Ni-rich sites whether hydrogen is at grain boundary or in the crystal. This feature is also found in other theoretical work[28] when hydrogen atoms are present in the crystalline Ni_3Al. From Table I, it can be also found that the lowest formation energy when hydrogen takes the site in the region of grain boundary is much lower than that when hydrogen takes the site in the crystal. It can be predicted that hydrogen prefers to segregate

TABLE I. The impurity formation energy E_{imp} (in eV), the nearest-neighboring (NN) atoms, and the distance d_{NN} (in Å) between hydrogen and its NN atoms, when hydrogen occupies different sites $X0$–$X5$ in polycrystalline Ni_3Al. Here the $X0$ is the occupation site in the crystalline and $X1$–$X5$ are the sites in the grain boundary.

H occupation site		$X0$	$X1$	$X2$	$X3$	$X4$	$X5$
Model A	NN	Al_1	Ni_1	Ni_1	$Ni_{1,6,8,13}, Al_{11}$	Ni_{23}	Ni_{23}
	d_{NN}	1.59	1.63	1.49	1.79	1.68	1.66
	E_{imp}	−2.646	−4.172	−4.322	−3.107	−4.052	−3.388
Model B	NN	Ni_1	Ni_1	$Ni_{1,11}$	$Ni_{1,11,13}, Al_{6,8}$	Ni_{23}	Ni_{41}
	d_{NN}	1.59	1.58	1.62	1.79	1.46	1.66
	E_{imp}	−3.960	−3.392	−5.792	−3.351	−5.626	−3.947

at Ni-rich grain boundary. So the action of hydrogen at the grain boundary plays an important role in the embrittlement of Ni_3Al.

B. Interatomic energy

In order to investigate the interaction between adjacent atoms, the interatomic energies defined by Eq. (3) are calculated and some main results are listed in Tables II and III. When hydrogen occupies the $X1$ site, H atom forms a strong bonding with its nearest-neighboring (NN) Ni_1 atom ($E^A_{H_1-Ni_1}=-2.518$ eV and $E^B_{H_1-Ni_1}=-2.674$ eV, the superscript italic A and B indicate the case in models A and B, respectively), and the bonding strength is comparable to that of boron with its adjacent atoms in the same Ni_3Al grain boundary ($E_{B-Ni_1}=-2.608$ eV).[37] However, the bonding formed between hydrogen and its next-nearest-neighboring (NNN) and other neighboring atoms are much weaker, for example, $E^B_{H_1-Ni_{2,3,4,5}}=-0.638$ eV, and $E^B_{H_1-Ni_{19,20}}=-0.305$ eV. The space of the void of the capped prism at which $X1$ locates is the largest in the $\Sigma 13$ grain boundary. When boron occupies this void, boron almost locates at the center of this void, and forms strong bonding with its neighboring atoms ($E_{B-Ni_{2,3,4,5}}=-2.009$ eV, ($E_{B-Ni_{19,20}}=-2.962$ eV), so boron acts as a ''bridge'' and increases the cohesive strength of Ni_3Al grain boundaries.[37] On the contrary, hydrogen cannot act as a ''bridge'' and cannot strengthen the grain boundary in Ni_3Al, when it occupies the $X1$ site.

It can be found from Tables II and III that the bonding strength between host metal atoms, which are the neighboring atoms of hydrogen, is weakened. Especially when hydrogen occupies $X2$ sites, the interatomic energy is increased by 0.602 eV for the most weakened bond Ni_1-$Al_{11,12}$ in model A and by 0.888 eV for Ni_1-$Ni_{11,12}$ in model B (noting that the interatomic energy is lower, the bond is stronger). On the other hand, we should pay attention to the direction of bondings. Many bonds (such as Ni_1-$Al_{11,12}$, $Ni_{2,4}$-Al_{11}, and $Ni_{3,5}$-Al_{12} when H occupies the $X2$ site, and Al_{10}-$Ni_{13,14}$ and Al_{10}-$Ni_{15,17,16,18}$ when H occupies the $X4$ site in model A; and Ni_1-$Ni_{11,12}$, $Ni_{2,4}$-Ni_{11} and $Ni_{3,5}$-Ni_{12} when H occupies the $X2$ site, and Ni_{23}-Ni_{35} and Ni_{24}-Ni_{36} when H occupies the $X4$ site in model B) which are almost perpendicular to the grain boundary, are weakened by hydrogen. Nevertheless, most of the strongest bondings between hydrogen and

TABLE II. The interatomic energy E_{lm} (in eV) for the typical pairs of atoms l and m, when hydrogen occupies the $X1$, $X2$, and $X4$ sites, respectively, in model A. $\Delta E_{lm}=E_{lm}$ (GBXn)-E_{lm} (GB) (in eV) is the change of interatomic energy induced by the presentation of hydrogen.

Pair of atoms	GB	GB$X1$		GB$X2$		GB$X4$	
l-m	E_{lm}	E_{lm}	ΔE_{lm}	E_{lm}	ΔE_{lm}	E_{lm}	ΔE_{lm}
Ni_1-Ni_2	−1.441	−1.236	0.205	−0.901	0.540	−1.431	0.010
Ni_1-Al_{11}	−1.192	−1.165	0.027	−0.590	0.602	−1.189	0.003
Ni_2-Al_{11}	−2.284	−2.306	−0.022	−2.007	0.277	−2.255	0.029
$Al_{10}-Ni_{13}$	−0.587	−0.598	−0.011	−0.596	−0.009	−0.325	0.262
$Al_{10}-Ni_{15}$	−1.230	−1.228	0.002	−1.216	0.014	−1.060	0.170
$Al_{10}-Ni_{23}$	−1.282	−1.298	−0.016	−1.301	−0.019	−1.053	0.229
$Ni_{15}-Ni_{23}$	−2.384	−2.389	−0.005	−2.377	0.007	−1.931	0.453
H_1-Ni_1		−2.518		−2.317		0.000	
H_1-Ni_2		−0.616		−1.176		0.000	
H_1-Al_{10}		0.000		0.000		−0.385	
H_1-Al_{11}		0.050		−0.899		0.000	
H_1-Ni_{13}		0.000		0.000		−1.287	
H_1-Ni_{19}		−0.343		−0.505		0.000	
H_1-Ni_{23}		0.000		0.000		−1.931	
H_1-H_2				−0.182		0.000	

TABLE III. The interatomic energy E_{lm} (in eV) for the typical pairs of atoms l and m, when hydrogen occupies the $X1$, $X2$, and $X4$ sites, respectively, in model B. $\Delta E_{lm}=E_{lm}$ (GBXn)-E_{lm} (GB) (in eV) is the change of interatomic energy induced by the presentation of hydrogen.

Pair of atoms	GB	GB$X1$		GB$X2$		GB$X4$	
l-m	E_{lm}	E_{lm}	ΔE_{lm}	E_{lm}	ΔE_{lm}	E_{lm}	ΔE_{lm}
Ni_1-Ni_2	−1.386	−1.120	0.266	−0.952	0.434	−1.376	0.010
Ni_1-Ni_{11}	−1.664	−1.672	−0.008	−0.776	0.888	−1.644	0.020
Ni_2-Ni_{11}	−1.778	−1.805	−0.027	−1.171	0.607	−1.804	−0.026
$Ni_{15}-Ni_{23}$	−2.023	−2.024	−0.001	−2.035	−0.012	−1.440	0.583
$Ni_{15}-Ni_{35}$	−2.346	−2.318	0.028	−2.340	0.006	−2.160	0.186
$Ni_{23}-Ni_{35}$	−1.836	−1.860	−0.024	−1.821	0.015	−1.081	0.755
H_1-Ni_1		−2.674		−1.745		0.000	
H_1-Ni_2		−0.638		−1.267		0.000	
H_1-Ni_{10}		0.000		0.000		−0.336	
H_1-Ni_{11}		0.075		−1.833		0.000	
H_1-Ni_{13}		0.000		0.000		−0.669	
H_1-Ni_{19}		−0.305		−0.868		0.000	
H_1-Ni_{23}		0.000		0.000		−2.604	
H_1-H_2				−0.010		0.000	

host metal atoms (such as H_1-Ni_1, H_1-$Ni_{2,4}$, and H_2-$Ni_{3,5}$ when H occupies the $X2$ site; and H_1-Ni_{23}, H_2-Ni_{24}, when H occupies the $X4$ site, etc.) are almost parallel to the grain boundary. It is evident that only the bonds which are perpendicular to the grain boundary contribute strongly to the cohesive strength of the grain boundaries. Thus, the overall effect of hydrogen is to reduce the strength of the grain boundary in Ni_3Al. The grain boundaries in Ni_3Al are originally weak link,[4,5] the strength of the grain boundary will be weakened further when hydrogen presents in the grain boundary. It can be expected that the ultimate strength would be reduced by the appearance of hydrogen in the grain boundary. This is confirmed by the work of George *et al.* (680 MPa in oxygen, but 392 MPa in air).[4]

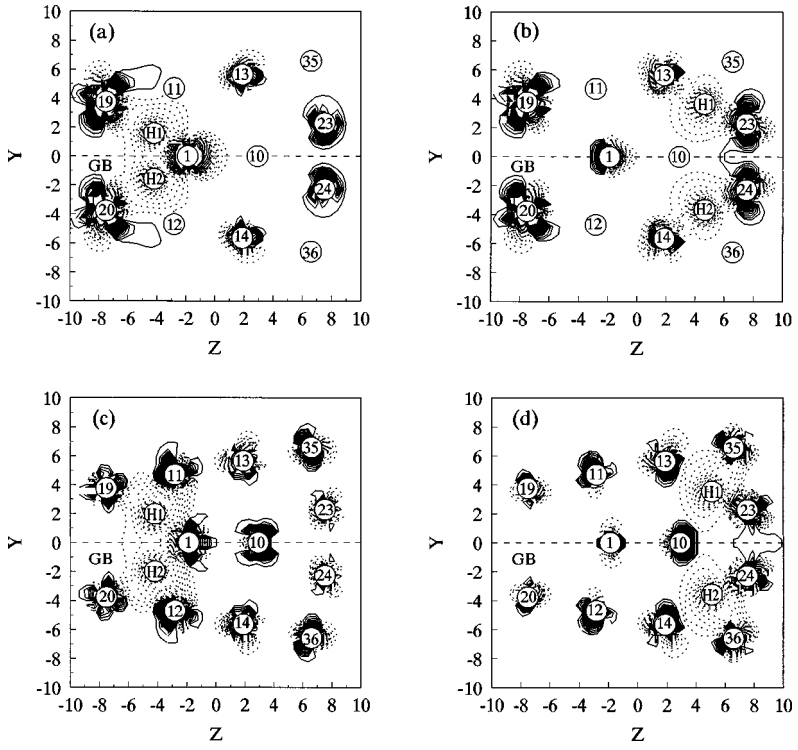

FIG. 2. The electron-density difference between the H-containing grain boundary and a superposition of H atom(s) and clean grain boundary. (a) and (b) for the situations when hydrogen occupies $X2$ and $X4$ sites, respectively, in model A. (c) and (d) for the situations when hydrogen occupies $X2$ and $X4$ sites, respectively, in model B. The circled numbers, which correspond to those in Fig. 1, indicate the position of atoms in the YZ plane. The contour spacings are 0.001e (a.u.)$^{-3}$. Solid lines indicate a gain of electron and dashed lines indicate a loss of electron.

When hydrogen atoms occupy the $X2$ sites, the two hydrogen atoms will interact with each other, the interatomic energy is $E^{A}_{H_1-H_2}=-0.182$ eV and $E^{B}_{H_1-H_2}=-0.010$ eV, respectively. This can be considered as the origin of a high concentration of hydrogen in the grain boundary. From the point of view of energy, hydrogen atoms prefer to occupy $X2$ sites, because of the lowest formation energy at this site. This indicates that hydrogen atoms tend to concentrate at this region in the Ni_3Al grain boundary and reduce the bonding strength between host metal atoms. As a result, the strength of the Ni_3Al grain boundary will be much weakened when the hydrogen concentration in the grain boundary is increased.

The occupation site of hydrogen can be further discussed from the calculated results of interatomic energy. Pay attention to the difference of the coordinate of $X2$ in these two models, in model A, the No. 11 atom is Al, the interatomic energy and distance for H_1-Al_{11} are -0.899 eV and 1.81 Å, respectively; in model B, the No. 11 atom is Ni, the interatomic energy and distance for H_1-Ni_{11} are -1.833 eV and 1.61 Å. It is evident that H will move towards the Ni_{11} atom when the No. 11 atom site is occupied by Ni instead of Al. It is more stable when H occupies the $X2$ site in model B than in model A, because the surrounding atoms of site $X2$ in model B are all Ni atoms, but there is a neighboring Al atom in model A.

C. Charge distribution

The electron-density difference is obtained by subtracting the electron density of the clean grain boundary and free hydrogen atom(s) from that of hydrogen-containing grain boundary (GB), so that the hydrogen-induced charge redistribution can be seen clearly. The calculated results show that the features of electron-density differences are very similar to each other when H occupies different sites, here only the electron density difference of the two most stable configuration GB$X2$ and GB$X4$ are shown in Fig. 2. The plotted planes are the YZ cut $(X=0)$ which are across the grain boundary and contains the hydrogen atom. It is clear that the electron density around the impurity hydrogen is decreased by the introduction of hydrogen. This is contrary to the case of boron in the Ni_3Al grain boundary.[37] This feature was also found in bulk Ni_3Al by the use of FPLMTO calculations.[28] The reduction of electron density in the interstitial region (hydrogen atoms occupy the interstitial sites) means the decreasing of bond strength between host metal atoms. This is consistent with the interatomic energy calculation. On the other hand, the charge distribution in the intermediate region of atoms, which is not nearby hydrogen, is hardly affected by hydrogen. This is similar to the case of boron in Ni_3Al grain boundary.[37]

IV. CONCLUSION

We have studied the effect of hydrogen in the polycrystalline Ni_3Al using first-principles numerical calculations. It is found that hydrogen atoms prefer to segregate at the grain boundaries, and occupy the Ni-rich interstitial holes, when hydrogen atoms are present in polycrystalline Ni_3Al. The equilibrium positions of H atoms are not in the center of these holes, instead, the hydrogen atom tends to locate near a certain atom and interacts strongly with it, but less with other atoms. Furthermore, the bonding strength between host atoms, which are near H atoms, is reduced evidently by the presentation of hydrogen. It can be concluded that the overall effect of H is to decrease the cohesive strength of Ni_3Al grain boundaries and make the intergranular fracture easier.

ACKNOWLEDGMENTS

We are grateful to Professor J.-M. Li and Dr. J.-L. Yang for their beneficial discussion. This work was supported by the National Natural Science Foundation of China.

[1] K. Aoki and O. Izumi, J. Jpn. Inst. Met. **43**, 1190 (1979).
[2] C. T. Liu, Scr. Metall. Mater. **27**, 25 (1992).
[3] E. P. George, C. T. Liu, and D. P. Pope, Scr. Metall. Mater. **27**, 365 (1992).
[4] E. P. George, C. T. Liu, and D. P. Pope, Scr. Metall. Mater. **28**, 857 (1993).
[5] E. P. George, C. T. Liu, and D. P. Pope, Scr. Metall. Mater. **30**, 37 (1994).
[6] E. P. George, C. T. Liu, and D. P. Pope, in *Structural Intermetallics*, edited by R. Darolia, J. J. Lewandowski, C. T. Liu, P. L. Martin, D. B. Miracle, and M. V. Nathal (The Minerals, Metals and Materials Society, 1993), p. 431.
[7] J. P. Hirth, Metall. Trans. A **11**, 861 (1980).
[8] R. M. Latanision, in *Atomistics of Fracture*, edited by R. M. Latanision and J. R. Pickens (Plenum, New York, 1983), p. 3.
[9] A. R. Troiano, Trans. Am. Soc. Met. **52**, 54 (1960).
[10] R. A. Oriani and P. H. Josephic, Acta Metall. **22**, 1065 (1974).
[11] C. Beachem, Metall. Trans. A **3**, 437 (1972).
[12] I. M. Robertson and H. K. Birnbaum, Acta Metall. **34**, 353 (1986).
[13] S. P. Lynch, Scr. Metall. **13**, 1051 (1979).
[14] G. M. Bond, I. M. Bobertson, and H. K. Birnbaum, Acta Metall. **37**, 1407 (1989).
[15] N. Masahashi, T. Takasugi, and O. Izumi, Metall. Trans. A **19**, 353 (1988).
[16] N. Masahashi, T. Takasugi, and O. Izumi, Acta Metall. **36**, 1823 (1988).
[17] X. J. Wan, J. H. Zhu, and K. L. Jing, Scr. Metall. Mater. **26**, 473 (1992).
[18] X. J. Wan, J. H. Zhu, and K. L. Jing, Scr. Metall. Mater. **26**, 479 (1992).
[19] A. K. Kuruvilla and N. S. Stoloff, Scr. Metall. **19**, 83 (1985).
[20] H. X. Li and T. K. Chaki, Acta Metall. Mater. **41**, 1979 (1993).
[21] H. X. Li and T. K. Chaki, Mater. Sci. Eng. A **192/193**, 387 (1995).
[22] Y. Tong and J. F. Knott, Scr. Metall. Mater. **25**, 1651 (1991).
[23] M. E. Eberhart, K. H. Johnson, R. P. Messmer, and C. L. Briant, in *Atomistics of Fracture*, edited by R. M. Latanision and J. R. Pickens (Plenum, New York, 1983), p. 255.
[24] M. E. Eberhart, R. M. Latanision, and K. H. Johnson, Acta Metall. **33**, 1769 (1985).

[25] D. Tománek, Z. Sun, and S. G. Louie, Phys. Rev. B **43**, 4699 (1991).
[26] W. Zhong, Y. Cai, and D. Tománek, Nature (London) **362**, 435 (1993).
[27] C. L. Fu and G. S. Painter, J. Mater. Res. **6**, 719 (1991).
[28] S. N. Sun, N. Kioussis, S. P. Lim, A. Gonis, and W. H. Gourdin, Phys. Rev. B **52**, 14 421 (1995).
[29] D. E. Ellis and G. S. Painter, Phys. Rev. B **2**, 2887 (1970).
[30] E. J. Baerends, D. E. Ellis, and P. Ros, Chem. Phys. **2**, 41 (1973).
[31] F. W. Averill and D. E. Ellis, J. Chem. Phys. **59**, 6412 (1973).
[32] B. Delley, D. E. Ellis, A. J. Freeman, E. J. Baerends, and D. Post, Phys. Rev. B **27**, 2132 (1983).
[33] D. E. Ellis, G. A. Benesh, and E. Byrom, Phys. Rev. B **16**, 3308 (1977).
[34] D. Guenzburger and D. E. Ellis, Phys. Rev. B **45**, 285 (1992).
[35] U. Von Barth and L. Hedin, J. Phys. C **5**, 1629 (1972).
[36] C.-Y. Wang, F. An, B.-L. Gu, F.-S. Liu, and Y. Chen, Phys. Rev. B **38**, 3905 (1988).
[37] F.-H. Wang, C.-Y. Wang, and J.-L. Yang, J. Phys.: Condens. Matter **8**, 5527 (1996).
[38] S. P. Chen, A. F. Voter, and D. J. Srolovitz, Scr. Metall. **20**, 1389 (1986).
[39] M. I. Baskes, C. F. Melius, and W. D. Wilson, in *Hydrogen Effects in Metals,* edited by I. M. Bernstein and A. W. Thompson (A. I. M. E., New York, 1980), p. 67.
[40] S. M. Myers, S. T. Picranx, and R. E. Stoltz, J. Appl. Phys. **50**, 5710 (1979).